Kinetics and Mechanism of 4-Acetoxytoluene Oxidation by Ozone in an Acetic Anhydride Solution in the Presence of Manganese Bromide Catalysts

A. G. Galstyan and A. A. Sedykh

East Ukrainian National University, Institute of Chemical Technologies, Rubezhnoe, Ukraine
e-mail: annasedych@mail.ru

Received June 9, 2008

Abstract—The kinetics of the reaction of ozone with 4-acetoxytoluene in an acetic anhydride solution in the presence of a manganese bromide catalyst is reported. Under these conditions, the major reaction products are 4-acetoxybenzylidenediacetate (68.0%), 4-acetoxybenzyl acetate (18.5%), and 4-acetoxybenzyl bromide (1.6%). The effect of manganese(II) acetate and potassium bromide on the selectivity of oxidation at the methyl group has been investigated. A probable redox catalysis mechanism explaining the experimental data is considered.

INTRODUCTION

It was shown earlier [1] that the oxidation of 4-acetoxytoluene (4-AT) by ozone at low temperatures (5–10°C) in acetic anhydride in the presence of manganese(II) acetate and an acylation catalyst (sulfuric acid) yields 4-acetoxybenzyl acetate (4-ABA) as the main product (63.3%). It has been impossible to stop the process at deeper oxidation stages and to isolate, for example, 4-acetoxybenzylidene diacetate (4-ABDA) as the major product.

To solve this problem, in the present work we studied the influence of potassium bromide on the kinetics and product composition of the catalytic oxidation of 4-AT by ozone for the reason that alkali metal bromides were reported earlier to accelerate the catalytic oxidation of methylbenzenes by ozone [2].

EXPERIMENTAL

Acetic anhydride (analytical grade) was used without further purification. Chromatographically pure 4-AT was prepared by the acylation of 4-hydroxytoluene (4-HT) [3] followed by recrystallization from water. 4-ABA and 4-ABDA were synthesized according to standard procedures [4, 5]. Manganese(III) acetate and its mixture with potassium bromide were prepared under the conditions of complete manganese(II) acetate ozonation in an acetic anhydride solution. Ozone was synthesized from air under barrier discharge conditions [6].

The kinetics and oxidation product composition were studied in a temperature-controlled column (0.02 l) fitted with a fine- pored glass plate for distribution of the ozone–air mixture flow. The gas mixture containing 4×10^{-4} mol/l ozone was fed into the reaction zone at a rate of 30 l/h.

For determination of the rate constants of the reaction of ozone with 4-AT and products of its oxidation, the ozone–air mixture was continuously passed through a temperature-controlled shaker reactor (0.1 l) containing acetic anhydride as the solvent. After the solvent was saturated with ozone, a certain volume of a substrate solution was introduced. The gaseous and liquid phases were mixed by shaking the reactor at a rate ensuring kinetic control of the reaction (>8 shakes per second).

Apparent rate constants were derived from ozone concentration profiles (Fig. 1) using the formula suggested in [6]:

$$k_{app} = \frac{\omega([O_3]_0 - [O_3]_{fin})}{\alpha[O_3]_{fin}^n [ArH]_0^m},$$

where k_{app} is the apparent rate constant taking into account all directions of attack by ozone (l mol^{-1} s^{-1}), w is the gas flow rate (l/s), α is the Henry coefficient, $[ArH]_0$ is the initial concentration of the substrate (mol/l), $[O_3]_0$ and $[O_3]_{fin}$ are the ozone concentrations in the gas phase before and after the reactor (mol/l), and n and m are the reaction orders with respect to the reacting compounds ($n = m = 1$, as determined under the conditions of our experiments).

The ozone uptake was determined from the ozone concentration profiles (Fig. 1) using the formula

$$\Delta O_3 = \omega \left([O_3]_0 \tau - \int_0^\tau [O_3]_{fin} d\tau\right), \text{ mol.}$$
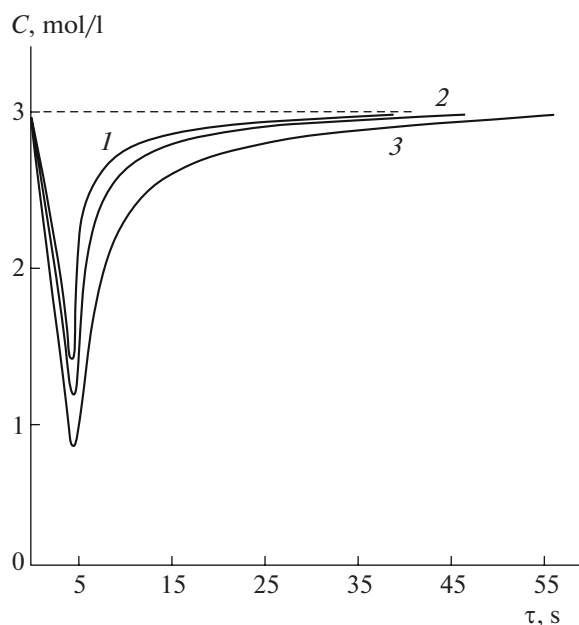
Fig. 1. Ozone concentration profiles for 4-AT oxidation by ozone in acetic anhydride at (*1*) 15, (*2*) 20, and (*3*) 40°C.

Fig. 2. Kinetics of 4-AT oxidation by ozone in acetic anhydride in the presence of manganese(II) acetate and potassium bromide at 5°C: (*1*) 4-AT, (*2*) 4-ABDA, (*3*) 4-ABA, (*4*) 4-ABAC, (*5*) 4-ABB, and (*6*) $Mn^{2+}Br^{\cdot}$ (the arrow indicates the ozone shutoff point). $[4\text{-}AT]_0 = 0.4$ mol/l, $[O_3]_0 = 4 \times 10^{-4}$ mol/l, $[H_2SO_4]_0 = 1.2$ mol/l, $[Mn(OAc)_2]_0 = 0.1$ mol/l, and $[KBr]_0 = 0.1$ mol/l. The specific flow rate of the ozone–air mixture is 0.37 s^{-1}.

The integral was calculated graphically, using Simpson's rule in the estimation of the areas of curvilinear figures [7].

The stoichiometric coefficient of ozone was calculated as

$$n = \Delta O_3/\Delta ArH, \text{ mol,}$$

where ΔArH is the reactant consumption equivalent to the ozone uptake ΔO_3.

The rate constants of the reactions of 4-AT and its conversion products with $Mn^{2+}Br^{\cdot}$ were derived from the initial portions of reactant consumption curves.

The concentrations of 4-AT and its oxidation products in the solution were determined by GLC [8].

RESULTS AND DISCUSSION

The ozonation of 4-AT in acetic anhydride catalyzed by sulfuric acid, manganese(II) acetate, and potassium bromide at 5°C yields 4-ABDA as the major oxidation product (68.0%) (Fig. 2). The reaction mixture also contains 4-ABA in 18.5% yield, 4-acetoxybenzyl bromide (4-ABB) (1.7%), and 4-acetoxybenzaldehyde (4-AB), whose concentration in the solution does not exceed 10^{-4} mol/l. The complete oxidation of 4-AT results in the accumulation of 4-acetoxybenzoic acid (4-ABAC) in the system. The ozone consumption is close to 2 mol per mole of the substrate. No oxidation of 4-AT by dioxygen occurs without ozone.

After a short induction period, 4-ABAC and 4-ABDA form at a constant rate. When 4-AT is introduced into the system containing manganese in the active form $Mn^{2+}Br^{\cdot}$ [4], the formation of the reaction
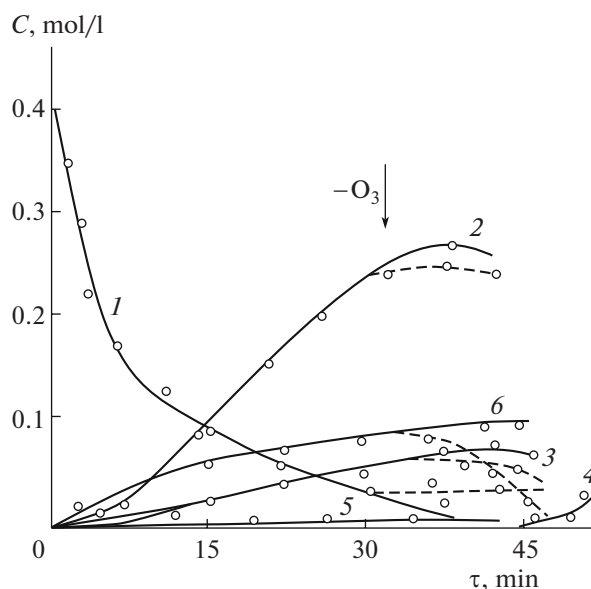
products begins without an induction period and the concentration of the active form of the catalyst first decreases rapidly to 0.01 mol/l and then increases as the substrate is consumed, as in the previous experiment (Fig. 2, curve *6*). Ozone should be supplied continuously. The cessation of ozone supply to the system stops the process: the oxidation of 4-AT and accumulation of the reaction products cease rapidly, and trivalent manganese passes into the divalent state (Fig. 2). The initial rate of the catalytic oxidation reaction depends linearly on the reactant concentrations. It is first-order with respect to the catalyst, substrate, and ozone and is independent of the dioxygen concentration (Fig. 3):
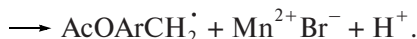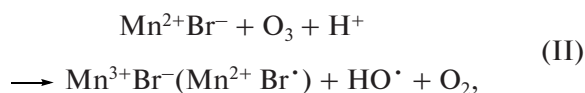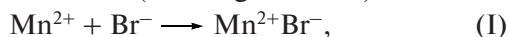
$$W = [AcOArCH_3]_0[O_3]_0[Mn^{2+}]_0[Br^-]_0.$$

The results obtained for the oxidation of 4-AT in the presence of manganese bromide catalysts of different compositions are presented in Table 1. It can be seen that the initiation of selective oxidation at the methyl group with manganese(II) acetate in the absence of bromide ions mainly yields 4-ABA and the 4-ABDA yield does not exceed 14.0% even at high catalyst concentrations (0.18 mol/l). Potassium bromide increases the depth of selective oxidation and substantially decreases the optimal manganese(II) acetate concentration. The maximum selectivity of 4-AT oxidation is achieved at comparable substrate and catalyst concentrations and $[Mn^{2+}]/[Br^-] = 1 : 1$ (Table 1). A further increase in the potassium bromide or manga-

nese salt concentration exerts no effect on the selectivity of oxidation. According to published data [4, 5], the increase in the catalytic activity of manganese(II) acetate in the presence of potassium bromide is likely due to the formation of the highly active metal bromide complex $Mn^{2+}Br^{\bullet}$.

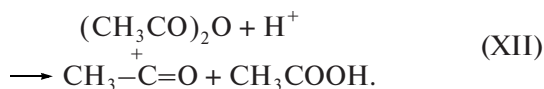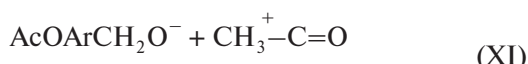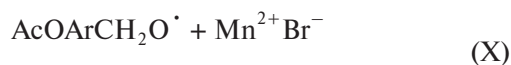Let us consider the above kinetic data in terms of the classical scheme of an unbranched chain reaction.
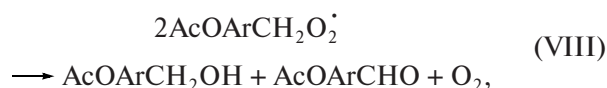
Catalytic initiation (radical generation):

$$Mn^{2+} + Br^- \longrightarrow Mn^{2+}Br^-, \qquad (I)$$

$$Mn^{2+}Br^- + O_3 + H^+ \qquad (II)$$
$$\longrightarrow Mn^{3+}Br^-(Mn^{2+}Br^{\bullet}) + HO^{\bullet} + O_2,$$

$$Mn^{2+}Br^{\bullet} + AcOArCH_3 \qquad (III)$$
$$\longrightarrow AcOArCH_2^{\bullet} + Mn^{2+}Br^- + H^+.$$

Chain propagation:

$$AcOArCH_2^{\bullet} + O_2 \longrightarrow AcOArCH_2O_2^{\bullet}, \qquad (IV)$$

$$AcOArCH_2O_2^{\bullet} + O_3 \longrightarrow AcOArCH_2O^{\bullet} + 2O_2, \quad (V)$$

$$AcOArCH_2O_2^{\bullet} + AcOArCH_3 \qquad (VI)$$
$$\longrightarrow AcOArCH_2OH + AcOArCH_2^{\bullet},$$

$$AcOArCH_2O_2^{\bullet} + Mn^{2+}Br^- + H^+ \qquad (VII)$$
$$\longrightarrow AcOArCH_2O_2H + Mn^{2+}Br^{\bullet}.$$

Chain termination:

$$2AcOArCH_2O_2^{\bullet} \qquad (VIII)$$
$$\longrightarrow AcOArCH_2OH + AcOArCHO + O_2,$$

$$2AcOArCH_2O_2^{\bullet} \longrightarrow 2AcOArCH_2O^{\bullet} + O_2, \qquad (IX)$$

$$AcOArCH_2O^{\bullet} + Mn^{2+}Br^- \qquad (X)$$
$$\longrightarrow AcOArCH_2O^- + Mn^{2+}Br^{\bullet},$$

$$AcOArCH_2O^- + CH_3\overset{+}{-}C=O \qquad (XI)$$
$$\longrightarrow AcOArCH_2OCOCH_3,$$

$$(CH_3CO)_2O + H^+ \qquad (XII)$$
$$\longrightarrow CH_3\overset{+}{-}C=O + CH_3COOH.$$

At the initial point in time, when the system contains almost no oxidation products, active species result from reactions (I) and (II) and radicals are generated in reaction (III). Continuous ozone supply to the system makes it possible to maintain a rather high concentration of the active form of the $Mn^{2+}Br^{\bullet}$ catalyst and, accordingly, a high acetoxybenzyl radical (ABR) formation rate (Table 2).

At $[O_2]_0 \gg [O_3]_0 \approx 2 \times 10^2$ mol/l, the resulting radicals turn into acetoperoxide radicals (APRs) (reaction (IV)), whose further conversion in terms of the above scheme is possible when $W_i = W_t \ll W_p$, i.e., the chain length is $v = W_{exp}/W_i \gg 1$. However, estimates
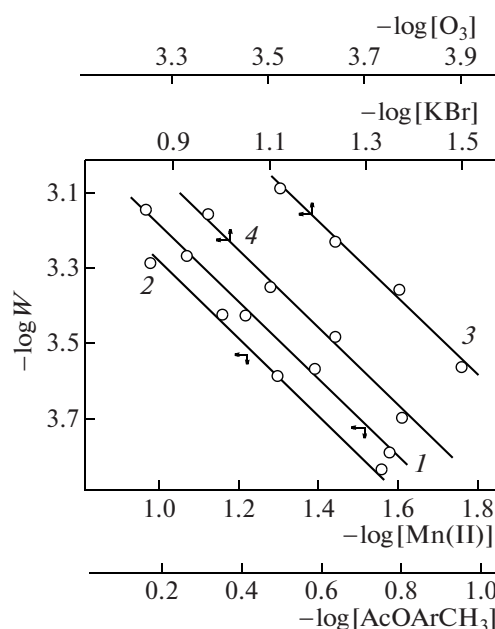
Fig. 3. Dependences of the 4-AT oxidation rate on the concentration of (*1*) manganese(II) acetate, (*2*) substrate, (*3*) potassium bromide, and (*4*) ozone.

demonstrated that these conditions are not fulfilled in our experiments: $W_i(W_3) = W_t(W_9) \gg W_p(W_5; W_6; W_7)$, and the chain length is $v = W_{exp}/W_i = 9.5 \times 10^{-4}/12.4 \times 10^{-4} = 0.8$. It is most likely that, under these conditions, 4-AT is predominantly oxidized via a radical–ion nonchain mechanism in which the oxidation products result mainly from the decay of APRs.

The peroxide radicals decay predominantly via reaction (IX) since the occurrence of reaction (VIII) would imply the parallel formation of 4-ABA and 4-ABDA, contrary to the experimental data: it can be

Table 1. Effect of the concentration of the manganese bromide catalyst of different compositions on the 4-ABDA and 4-ABA yields

$[Mn(OAc)_2]_0$, mol/l	$[KBr]_0$, mol/l	4-ABDA yield, %	4-ABA yield, %
0.18	–	14.0	63.3
0.10	–	13.8	42.3
0.10	0.04	20.0	9.0
0.10	0.08	45.1	12.1
0.10	0.10	68.0	18.5
0.08	0.10	45.0	12.3
0.04	0.10	15.5	9.3
0.12	0.10	67.8	17.0
0.12	0.14	68.0	18.1

Note: $[4\text{-}AT]_0 = 0.4$ mol/l, $[H_2SO_4]_0 = 1.2$ mol/l, $[O_3]_0 = 4 \times 10^{-4}$ mol/l, $T = 5°C$.

Table 2. Kinetic parameters of the reactions of the catalytic cycle

Reaction	k^*, l mol^{-1} s^{-1}	E, kJ/mol	Reaction rate (W), mol l^{-1} s^{-1}
(II)	20.3 ± 2.0	22.1 ± 2.2	8.1×10^{-4}
(III)	$3.1 \times 10^{-2} \pm 0.3$	34.4 ± 3.5	12.4×10^{-4}
(IV)	4.7×10^9 (25°C)		1.3×10^{-2}
(V)	10^2 (20°C)		1.4×10^{-7}
(VI)	2.3		3.2×10^{-6}
(VII)	10^2		3.5×10^{-5}
(VIII)	10^8		12.4×10^{-4}
(IX)	10^8		12.4×10^{-4}
(X)	10^3		3.5×10^{-4}
(XIII)	$9.2 \times 10^{-3} \pm 0.9$	40.4 ± 4.0	3.7×10^{-4}
(XIV)	$4.9 \times 10^{-3} \pm 0.4$	47.5 ± 4.5	2.0×10^{-4}
(XV)	0.59 ± 0.05	20.3 ± 2.0	0.9×10^{-4}

Note: $[4\text{-}AT]_0 = 0.4$ mol/l, $[Mn(OAc)_3]_0 = 0.1$ mol/l, $[KBr]_0 = 0.1$ mol/l, $[H_2SO_4]_0 = 1.2$ mol/l, $[O_3]_0 = 4 \times 10^{-4}$ mol/l, $T = 5°C$; the reaction rate determined from the data presented in Fig. 2 (curve 1) is $W_{exp} = 9.5 \times 10^{-4}$ mol l^{-1} s^{-1}.

* k_2, k_3, and k_{12} were calculated from our data; the k_4 value is for the methyl radical [10]; k_5 is for the reaction $CH_3O_2^{\bullet} + O_3$ [11]; k_6, k_7, k_8, and k_9 are for the reaction of toluene with cobalt [12], corrected for the redox potential of Mn(II) [9]; $k_{10} = 10k_7$, considering the higher reactivity of the alkoxy radical [9]. The 4-APR concentration was estimated from the steady-state reactant concentration condition $k_3 [AcOArCH_3][Mn^{2+}Br^{\bullet}] = k_9 [AcOArCH_2O_2^{\bullet}]^2$; hence, $[AcOArCH_2O_2^{\bullet}] = ((k_3[AcOArCH_3][Mn^{2+}Br^{\bullet}])/k_9)^{1/2} = 3.52 \times 10^{-6}$ mol/l.

seen from Table 1 that the ozonation of 4-AT in acetic anhydride in the presence of the mineral acid and manganese(II) acetate yields 4-ABA and 4-ABDA in a 4 : 5 : 1 ratio. Evidently, the alkoxy radicals (ARs) formed in the solvent cage under our experimental conditions escape into the bulk (reaction (IX)) [9], where they react with the reduced form of the catalyst at a high rate (reaction (X)) to form the reaction products ($W_{10}/W_7 \approx 10$ [9]).

The 4-ABA formed via this scheme is likely oxidized in a similar way to produce 4-ABDA (reaction (XIII)) and then 4-ABAC (XIV), which is indicated by the kinetic parameters of the oxidation of 4-ABA and 4-ABDA (Table 2) and by the reaction product composition data (Fig. 2):
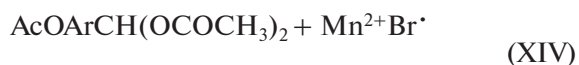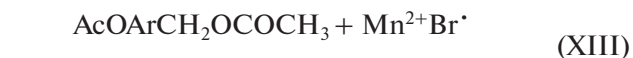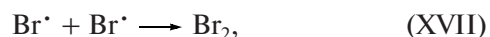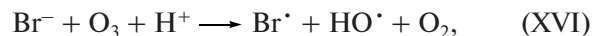
$$AcOArCH_2OCOCH_3 + Mn^{2+}Br^{\bullet} \quad \text{(XIII)}$$
$$\longrightarrow AcOArCH^{\bullet}OCOCH_3 + Mn^{2+}Br^- + H^+,$$

$$AcOArCH(OCOCH_3)_2 + Mn^{2+}Br^{\bullet} \quad \text{(XIV)}$$
$$\longrightarrow AcOArC^{\bullet}(OCOCH_3)_2 + Mn^{2+}Br^- + H^+.$$

Figure 2 (curve 6) shows that the concentration of the active form of manganese in the solution increases continuously with a decrease in the 4-AT concentration and reaches its maximum value (0.08 mol/l) at the point of complete substrate oxidation. This is due to the fact that, at the initial moment of the reaction, the rate of $Mn^{2+}Br^-$ oxidation by ozone (W_2) is somewhat lower than the rate of its reduction by the substrate

(W_3) (Table 2) and, as a consequence, the $Mn^{2+}Br^{\bullet}$ concentration in the system at the initial moment is low (the reaction mixture is light brown) (at $[O_3]_0 = 4 \times 10^{-4}$ mol/l and $[4\text{-}AT]_0 = 0.4$ mol/l, $[Mn^{2+}Br^-] = 0.07$ mol/l and $[Mn^{2+}Br^{\bullet}] = 0.03$ mol/l; $k_2 = 20.3$ l mol^{-1} s^{-1} and $k_3 = 3.1 \times 10^{-2}$ l mol^{-1} s^{-1} (Table 2); $W_2 = 8.1 \times 10^{-4}$ mol l^{-1} s^{-1} and $W_3 = 12.4 \times 10^{-4}$ mol l^{-1} s^{-1}). The $Mn^{2+}Br^{\bullet}$ reduction rate decreases with 4-AT consumption and the formation of less reactive 4-ABDA and 4-ABA (Table 2). Because of this, the equilibrium concentration of $Mn^{2+}Br^{\bullet}$ in the system increases (at the end of the oxidation, the solution becomes violet). At the initial moment, when the $Mn^{2+}Br^{\bullet}$ concentration in the solution is low, the minimum rate of 4-ABDA formation corresponds to the maximum rate of 4-AT oxidation (Fig. 2). Under these conditions, 4-AT is oxidized by ozone predominantly at the double bonds of the aromatic ring to form ozonides (reaction (XV)).

$$AcOArCH_3 + O_3 \longrightarrow \text{ozonolysis products}, \quad \text{(XV)}$$

$$Br^- + O_3 + H^+ \longrightarrow Br^{\bullet} + HO^{\bullet} + O_2, \quad \text{(XVI)}$$

$$Br^{\bullet} + Br^{\bullet} \longrightarrow Br_2, \quad \text{(XVII)}$$

$$AcOArCH_2^{\bullet} + Br_2 \longrightarrow AcOArCH_2Br + Br^{\bullet}. \quad \text{(XVIII)}$$

4-ABB appears in the system owing to reactions (XVI)–(XVIII), and molecular bromine was detected in the exit gas.

Table 3. Temperature effect on the selectivity and the yield of the reaction products of 4-AT oxidation by ozone in acetic anhydride

T, °C	Reaction products, mol/l		Total selectivity, %
	4-ABDA	4-ABA	
5	0.272	0.074	86.5
10	0.260	0.068	82.0
20	0.210	0.062	68.0
30	0.122	0.048	42.5

Note: $[4\text{-AT}]_0 = 0.4$ mol/l, $[O_3] = 4.0 \times 10^{-4}$ mol/l, $[H_2SO_4]_0 = 1.2$ mol/l, $[Mn(OAc)_2] = 0.1$ mol/l, $[KBr]_0 = 0.1$ mol/l.

The selectivity of 4-AT oxidation into 4-ABDA is temperature-dependent: as the temperature is raised, the selectivity of oxidation at the methyl group with 4-ABDA formation decreases (Table 3). It might seem that this is in conflict with the experimental data according to which the rate of selective oxidation (reaction (III)) increases more rapidly than the rate of ozonolysis (reaction (XIII)) ($E_3 = 34.4$ kJ/mol, $E_{15} = 20.3$ kJ/mol (Table 2)). However, kinetic studies of the interaction between ozone and the reaction products showed that these regularities are indeed possible because the rate of 4-ABDA oxidation to 4-ABAC (reaction (XIV)) increases with temperature more rapidly than the rate of reaction (XIII), the rate-limiting step in 4-ABDA formation (Table 2).

Thus, 4-HT can be selectively oxidized into 4-ABDA with ozone in acetic anhydride via preacylation and the introduction of a mixture of manganese(II) acetate and potassium bromide into the oxidation system. The ozonation of 4-AT is the radical–ion nonchain process, which is indicated by the following facts: the reaction is first-order with the respect to the reactants, the chain length is $v \approx 0.8$, the selectivity of oxidation at the methyl group reaches its maximum at comparable concentrations of the substrate and catalyst, the ozone consumption is close to 2 mol per mole of the substrate, and cessation of ozone sup-ply to the reaction zone results in the complete termination of the process and in the conversion of $Mn^{2+}Br^{\cdot}$ into $Mn^{2+}Br^{-}$. The major oxidation product is 4-ABDA. The depth of 4-AT oxidation is greater in the presence of bromine ions owing to the accumulation of the active complex $Mn^{2+}Br^{\cdot}$ in the system.

REFERENCES

1. Sedykh, A.A. and Galstyan, A.G., *Zh. Prikl. Khim.*, 2006, vol. 79, no. 1, p. 125 [*Russ J. Appl. Chem.* (Engl. Transl.), vol. 79, no. 1, p. 123].
2. Potapenko, E.V. and Galstyan, G.A., *Zh. Prikl. Khim.*, 2000, vol. 73, no. 7, p. 1218 [*Russ J. Appl. Chem.* (Engl. Transl.), vol. 73, no. 7, p. 1291].
3. Ingold, C.K., *Structure and Mechanism in Organic Chemistry*, Ithaca: Cornell Univ., 1969.
4. Sakota, K., Kamija, J., and Ohta, N., *Bull. Chem. Soc. Jpn.*, 1968, vol. 41, no. 3, p. 641.
5. Zakharov, I.V., Galetii, Yu.V., and Adamyan, V.A., *Kinet. Katal.*, 1988, vol. 29, no. 5, p. 1072.
6. Shereshovets, V.V., Shafikov, N.Ya., and Komissarov, V.D., *Zh. Fiz. Khim.*, 1980, vol. 54, no. 5, p. 1288.
7. Baryshnikov, S.V., Medvedev, R.B., and Fialkov, Yu.Ya., *Vychislitel'naya matematika v khimii i khimicheskoi tekhnologii* (Computational Mathematics in Chemistry and Chemical Engineering), Kiev: Vishcha Shkola, 1986.
8. Galstyan, A.G., Sedykh, G.O., and Galstyan, G.A., *Ukr. Khim. Zh.*, 2007, vol. 73, no. 5, p. 101.
9. Denisov, E.T., *Konstanty skorosti gomoliticheskikh zhidkofaznykh reaktsii* (Rate Constants of Homolytic Liquid-Phase Reactions), Moscow: Nauka, 1971.
10. Denisov, E.T., Mitskevich, N.I., and Agabekov, V.E., *Mekhanizm zhidkofaznogo okisleniya kislorodsoderzhashchikh soedinenii* (Mechanism of the Liquid-Phase Oxidation of Oxygen-Containing Compounds), Minsk: Nauka Tekhnika, 1975.
11. Galstyan, G.A., Tyupalo, N.F., and Razumovskii, S.D., *Ozon i ego reaktsii s aromaticheskimi soedineniyami* (Ozone and Its Reactions with Aromatic Compounds), Lugansk: VUNU, 2004.
12. Zakharov, I.V. and Galetii, Yu.V., *Neftekhimiya*, 1978, vol. 18, no. 4, p. 615.